Experimental Cell Research **273,** 73–84 (2002)
doi:10.1006/excr.2001.5414, available online at http://www.idealibrary.com on IDEAL®

Involvement of the Fungal Nuclear Migration Gene *nudC* Human Homolog in Cell Proliferation and Mitotic Spindle Formation

Min-Ying Zhang,* Ning-Na Huang,† Gary A. Clawson,‡ Stephen A. Osmani,† Weihua Pan,‡ Ping Xin,‡ Mohammed S. Razzaque,* and Barbara A. Miller*,†,§,[1]

**Department of Pediatrics, ‡Department of Experimental Pathology and The Gittlen Cancer Research Institute, and §Department of Biochemistry and Molecular Biology, The Pennsylvania State University College of Medicine, The Milton S. Hershey Medical Center, Hershey, Pennsylvania 17033; and †The Henry Hood Research Program, The Sigfried and Janet Weis Center for Research, Geisinger Clinic, Danville, Pennsylvania 17822*

Essential genes which are required for normal nuclear migration and play a role in developmental processes have been isolated from model genetic organisms. One such gene is *nudC* (*nu*clear *d*istribution *C*), which is required for positioning nuclei in the cytoplasm of the filamentous fungus *Aspergillus nidulans* and for normal colony growth. This gene is highly conserved, structurally and functionally, throughout evolution and the human homolog, *HnudC*, has been cloned. To study the function of *nudC* in higher eukaryotic cells, *HnudC* was downregulated by developing triple ribozyme constructs, consisting of two *cis*-acting ribozymes which liberate an internal *trans*-acting ribozyme targeted to *HnudC*. Efficient cleavage sites in *HnudC* mRNA were identified using a library selection technique and *HnudC*-targeted internal ribozymes were cloned into a triple ribozyme cassette. Triple ribozyme constructs were subcloned into an ecdysone-inducible expression vector and stably transfected into human embryonic 293 cells. Muristerone A induced expression of the *HnudC* ribozyme and produced specific reduction of *HnudC* mRNA. Downregulation of *HnudC* mRNA resulted in significant inhibition of cell proliferation in clones expressing the *HnudC*-targeted triple ribozyme, which was not observed in uninduced cells or cells transfected with vector alone. In induced cultures, many mitotic cells demonstrated defects in spindle architecture during mitosis. The most common defect observed was multiple mitotic spindle poles rather than the expected bipolar structure. These data demonstrate the fundamental importance of *HnudC* in eukaryotic cell proliferation and a functional role for *HnudC* in spindle formation at mitosis. © 2001 Elsevier Science

[1] To whom correspondence and reprint requests should be addressed at Henry Hood Research Program, Weis Center for Research, Geisinger Clinic, 100 North Academy Avenue, Danville, Pennsylvania 17822-2616. Fax: (570) 271-6701. E-mail: bamiller1@geisinger.edu.

***Key Words: A. nidulans; HnudC;* mitosis; nuclear migration gene; ribozyme.**

INTRODUCTION

Nuclear migration is a fundamental feature of biological processes, including separation of daughter nuclei during cytokinesis, movement of nuclei during fertilization, and interphase nuclear positioning [1, 2]. The study of model genetic organisms has recently provided much insight by identifying genes involved in nuclear migration and cell division. Heat-sensitive *nud* (*nu*clear *d*istribution) mutants have been discovered in *Aspergillus nidulans,* which prevent nuclear migration into the mycelium. *nud* colonies are severely restricted for growth and differentiation. In *A. nidulans,* more than 14 *nud* loci have been identified and six *nud* genes have been cloned [3]. *nudA* encodes cytoplasmic dynein heavy chain [4] and *nudG* encodes dynein light chain [5]. *nudK* encodes the actin-related protein Arpl, which is a component of the dynactin complex and involved in dynein-mediated functions [3]. The *nudF* gene encodes a regulator of an unknown aspect of dynein motor function [6], and it encodes a protein with significant sequence identity to the human *LIS-1* (Miller-Dieker lissencephaly-1) protein, which is required for proper neuronal migration during brain development [7–11]. *nudE* is a homolog of the nuclear distribution protein RO11 of *Neurospora crassa* [12], and NUDE homologs associate with LIS-1 and dynein [11–14]. The interaction of the higher eukaryotic homologs of these fungal nuclear migration genes, cytoplasmic dynein, dynactin, LIS-1, and *nudE,* with each other and with microtubules, has recently been shown to be of critical importance in mitosis and in cytokinesis [8–12, 15, 16].

nudC is an essential gene required for positioning nuclei in the cytoplasm of *A. nidulans* [17, 18] and for normal colony growth [17]. Deletion of *nudC* results in a more severe phenotype than other nuclear distribu-

0014-4827/01 $35.00
© 2001 Elsevier Science
All rights reserved.

tion mutants, profoundly affecting morphology and composition of the cell wall and resulting in lethality [18]. In addition to nuclear migration defects, spores grow spherically, the thickness of the cell wall is increased, wall polymer composition and actin distribution are abnormal, and cells eventually lyse. *nudC* has been shown to regulate the level of *nudF* posttranscriptionally [6], but the biochemical function of *nudC* is unknown. To further understand the role of fungal nuclear migration genes in higher eukaryotes, homologs of *nudC* have been studied. Human [19, 20], mouse [21], rat [22, 23], and *Drosophila* [24] *nudC* genes have been cloned and their proteins have M_rs of 45,000 by SDS–PAGE. The amino terminus of higher eukaryotic NUDC does not overlap with *A. nidulans* NUDC, which is a smaller protein with a predicted M_r of 22,000. However, the carboxy terminal 94 amino acids of the human clone are homologous to rat (98%), *Drosophila* (76%), and *A. nidulans* (67%), and the carboxy portions of human, rat, or *Drosophila nudC* can fully complement the nuclear movement defect and restore normal colony growth to the *A. nidulans nudC3* mutant [19, 22, 24]. These data demonstrate that *nudC* has been structurally and functionally conserved throughout evolution and suggest that it has been maintained for an essential function.

Immunohistochemical examination of human tissues provides evidence that HNUDC has a role in eukaryotic cell proliferation. HNUDC is highly expressed in proliferating cells, including basal esophageal and colonic mucosa, spermatocytes, immunoblasts, cortical thymocytes, and early bone marrow precursors, and the high level of HNUDC expression in normal proliferating cells declines during maturation [19, 25]. All cell lines examined thus far express large quantities of HNUDC and in growth factor-deprived cells, expression is enhanced in response to growth factor stimulation [19, 22]. In addition, the level of HNUDC protein is elevated over 50-fold in lysates of bone marrow aspirates from patients with acute lymphoblastic or acute myelogenous leukemia compared to normal bone marrow, suggesting that upregulation of expression of *HnudC* may be part of the leukemic process [26]. HNUDC expression is also high in: (1) nonproliferating tissues which contain secretory cells, including the Islets of Langerhans and adrenal cortex and medulla, suggesting that it may be required in the vesicular movement involved in secretion; and (2) in ciliated cells, suggesting a potential role in ciliary assembly or motility [25]. Little or no HNUDC was observed in most other tissues.

In this report, we constructed triple ribozymes to downregulate *HnudC* mRNA to study the functional role of *HnudC* in proliferation of higher eukaryotic cells. Ribozymes are catalytic RNA molecules that recognize their target RNA in a highly sequence-specific manner [27]. Triple ribozyme (TRz) constructs based on the initial design of Taira *et al.* [28] were developed which consist of two *cis*-acting ribozymes flanking an internal *trans*-acting hammerhead ribozyme, which is targeted to *HnudC*. The *cis*-acting ribozymes efficiently liberate the internal ribozyme, which can then cleave numerous target transcripts *in vivo.* Here, we utilized an ecdysone-inducible expression vector capable of expressing a triple ribozyme cassette containing *HnudC*-targeted internal ribozymes. We stably transfected human embryonic 293 cells with this construct. Upon induction, the *HnudC*-targeted ribozyme is expressed. Induction of *HnudC*-targeted ribozymes results in decreased levels of *HnudC* mRNA *in vivo* and a marked inhibition of cell division, producing dramatic abnormalities in mitotic spindles. These data demonstrate the critical requirement for *HnudC* in eukaryotic cell proliferation and a functional role for *HnudC* in mitotic spindle formation.

MATERIALS AND METHODS

Construction of the pSNIP ribozyme cassette. The pSNIP ribozyme cassette (Fig. 1) was prepared from two previously constructed parent double ribozymes, designated pClip and pChop [29–32]. Each triple ribozyme section contains a double internal targeted *trans*-acting ribozyme with a short 3′ poly(A) tail, which enhances stability within cells.

Library selection of target sites on HnudC mRNA. To select optimal target sites on *HnudC* mRNA for the *HnudC* ribozyme, a modification of the library selection technique of Lieber and Strauss [33, 34] was used. Briefly, a single-stranded DNA library (SSDNA) was created with a 5′ region of 16 fixed nucleotides containing the T7 promoter, a region of 6 random nucleotides, a -GA-, another region of 9 random nucleotides, and another distinct region of 15 fixed nucleotides at the 3′ end (16-N_6-GA-N_9-15). This SSDNA pool was used to construct a double-stranded DNA library (DSDNA) by PCR. The DSDNA was transcribed to make the RNA library. Target *HnudC* RNA was made by *in vitro* transcription using full-length human *nudC* cDNA as the template. An aliquot of the library RNA that contains approximately 1×10^9 different random sequences was added to *HnudC* RNA. After 20 min incubation in buffer (20 mM Tris–HCl, 2.5 mM $MgCl_2$) at 37°C, the reaction mixture was separated in an 8% polyacrylamide gel under nondenaturing conditions. Bound library RNAs were recovered with the target RNA and then converted to DNA by RT–PCR. This double-stranded DNA was transcribed into RNA again by T7 RNA polymerase. This procedure constitutes a "round" of selection. This was then repeated with the selected RNA library and target RNA until the binding of library to target RNA no longer increased; six rounds were sufficient. The selected transcripts, which were efficient in binding *HnudC* RNA, were amplified by PCR and cloned, and 60 clones were sequenced. Six-consensus potential high-affinity binding sites for *HnudC*-targeted ribozymes were identified which contained a -TC- internal site (see Table 1).

Construction and characterization of HnudC-targeted triple ribozymes. *HnudC*-targeted internal ribozymes were synthesized for the six identified cleavage sites as oligonucleotides, which contain the T7 promoter, the specific identified *HnudC* sequences, and the conserved active ribozyme core sequence (single internal ribozyme). Two different *HnudC* single ribozyme oligonucleotides were also annealed together to create double internal ribozymes (Fig. 1). These double internal ribozyme oligonucleotides, therefore, recognize two

different *HnudC* target sequences and contain two conserved active ribozyme cores. Both single and double oligonucleotides were then amplified by PCR using the primers 5′CCGAAGCTTAATACG3′ and 5′GACCCTTGGAATTC3′. The 91-bp (single) and 129-bp (double) PCR products were then transcribed into ribozyme RNA with T7 polymerase.

For target cleavage reactions, [^{32}P]CTP-labeled *HnudC* target RNA was prepared using *HnudC* cDNA as a template. Following transcription, the DNA template was removed by incubation with RNase-free DNase. The [^{32}P]CTP-labeled *HnudC* RNA and unlabeled single or double *HnudC* ribozymes were then incubated at molar ratio of 1:12.5 in buffer (20 mM Tris–HCl, 50 mM $MgCl_2$) at 37°C for 80 min. After the cleavage reaction, the mixture was separated on a 5% denatured polyacrylamide gel and detected with autoradiography. The DNA oligonucleotides of the most effective double ribozymes were then subcloned into pIND-SNIP at both *Bam*HI/*Eco*RI and *Bgl*II/*Mef*I sites.

For *in vitro* self-liberation analyses, 1–2 μg of the pSNIP-*HnudC* ribozyme DNA was cloned into the pCRII vector. A DNA template for *in vitro* transcription was produced from pCRII pSNIP *HnudC* (see below) with M13 primers, followed by transcription with Sp6 transcriptase and [^{32}P]CTP. After 5–50 min of incubation at 37°C, the ^{32}P-labeled mRNA was analyzed on a 6% polyacrylamide 8 M urea gel.

Isolation of stable cell lines transfected with HnudC triple ribozymes in the ecdysone-inducible vector. The ecdysone (muristerone A)-inducible expression system was used in this study (Invitrogen, Carlsbad, CA). To select stably transfected cell lines, 1×10^5 kidney embryonic 293 cells were seeded in 35-mm culture plates with 3 ml of Dulbecco's medium and incubated at 37°C for 24 h. Two micrograms of the regulatory plasmid DNA pVgRXR was gently mixed with 10 μg of lipofectin (GIBCO BRL) to form DNA–lipid complexes in serum-free medium. After 30 min, the complex was added to each well and the incubation continued for 12 h. The DNA containing serum-free medium was then replaced by the regular Dulbecco's and the transfected cells were allowed to recover for 40 h. Stably transfected cells expressing the pVgRXR were selected by adding zeocin to a final concentration of 200 μg/ml using the manufacturer's recommended protocol. The medium was changed every 3 days until single colonies were visible. Twenty clones were selected, expanded, and transfected with the reporter plasmid pIND/LacZ to test for muristerone-A-inducible gene expression. The optimal concentration of inducer was determined. Two micromolar muristerone A gave the maximal induction of LacZ in 293 cells. This concentration was used for all remaining experiments. The stable cell line, which showed the highest LacZ expression, was used as the parental cell line to isolate stable cell lines expressing *HnudC* ribozymes. A second transfection was then performed with pIND-SNIP containing *HnudC* ribozyme constructs A, D, E, or F (see Results) and double-stable cell lines were selected with both zeocin and G418 (600 μg/ml) using the methods described above. pIND-SNIP without any internal *HnudC* ribozymes was also transfected into parental cell lines and used as a control. Stable cell lines carrying both pVgRXR and pIND-SNIP-*HnudC* ribozymes were maintained in Dulbecco's media containing 10% fetal calf serum, penicillin/streptomycin, 200 μg/ml of zeocin, and 600 μg/ml of G418.

Viability assay. Five hundred 293 cells stably transfected with pIND-SNIP containing *HnudC* ribozyme constructs A, D, or E or control (see Results) were seeded in 24-well plates with 0.5 ml of medium containing both zeocin and G418. The plates were kept at 37°C for 24 h before muristerone A (2 μM final concentration) was added to each well. This was repeated daily because of instability of the inducer. In uninduced control wells, the same volume of carrier (ETOH) was added daily. The cell number was determined daily from days 5 to 11 after inducer addition. In representative experiments, nonadherent cells were also counted.

Analysis of apoptosis and cell cycle in ribozyme-induced cells. Cell lysates were prepared from induced and uninduced 293 cells and Western blotting performed as described previously [19]. Blots were probed with antibodies to poly(ADP-ribose) polymerase (PARP) (1/500, BD PharMingen, San Diego, CA), caspase 8 (1/500, BD PharMingen), and caspase 3 (1/1000, BD PharMingen). Secondary antibody was HRP-sheep antimouse Ig or HRP-donkey antirabbit Ig (caspase 3, Amersham) and detection was with ECL. For cell cycle analysis, cells were stained with propidium iodide and FACS analysis was used to measure the number of cells at G0–G1, G2–M, and S phases of the cell cycle.

Dot blot analysis. To confirm induction of *HnudC* ribozyme expression and determine the effect on *HnudC* mRNA levels, 1×10^5 293 cells stably transfected with pIND-SNIP containing *HnudC* ribozyme constructs A, D, and E (see Results) were seeded in 2 ml of Dulbecco's media and muristerone A (2 μM) was then added every 24 h. The cells were collected after 24, 48, and 72 h of incubation. Total RNA was purified from individual cell lines using TRI reagent (Molecular Research Center, Inc., Cincinnati, OH). Ten micrograms of each RNA was redissolved in 500 μl of ice-cold 10 mM NaOH, 1 mM EDTA and then blotted on zeta-probe GT blotting membranes using dot blot minifold (Schleicher & Schuell, Inc., Keene, NH). The membranes were hybridized by ExpressHyb hybridization solution (Clontech) under the manufacturer's recommended conditions. To detect *HnudC* ribozyme expression, the 447-bp *Hin*dIII/*Xba*I inserts from *HnudC* ribozyme A, D, or E were labeled using the Primer-a-Gene labeling system (Promega, Madison, WI). A 281-bp *Hin*dIII/*Xba*I insert from the pIND-SNIP vector without internal ribozyme was also labeled to detect expression of vector alone in control cells. *HnudC*-labeled cDNA was used as a probe to detect *HnudC* mRNA expression. All membranes were stripped and relabeled with a probe derived from glyceraldehyde-3-phosphate dehydrogenase (GPDH). Dots on the autoradiography were quantitated with Molecular Dynamics Densitometer (Huntington, NY).

Immunofluorescence of HnudC-targeted ribozyme expressing cells. Cells were grown in DMEM (Dulbecco's modified Eagle's media) supplemented with 10% fetal bovine serum, 200 μg/ml of zeocin, and 600 μg/ml of G418. Cells were grown on Nunc cover permanox chamber slides. Suppression of HNUDC was achieved by addition of 2 μM muristerone every 24 h for 3–7 days with addition of carrier alone acting as control. For immunofluorescence, cells were washed twice with PBS, fixed in 3% paraformaldehyde for 30 min, and permeabilized in 0.5% Triton X-100 in PBS for 5 min. Incubation for 30 min in 1% BSA/PBS preceded staining with primary antibody (anti-α-tubulin, monoclonal clone B-5-1-2, Sigma T-5168) for 1 h and secondary antibody (goat antimouse, Molecular Probes A-11029) for 45 min. Slides were also stained with DAPI to visualize DNA. Cells were viewed using a Nikon Eclipse E800 fluorescence microscope.

RESULTS

Construction of the HnudC-Targeted Ribozyme Cassette

HnudC-targeted triple ribozymes were prepared to study the function of *HnudC* in higher eukaryotic cells. We used the pSNIP cassette which combines two previous triple ribozyme cassettes, pClip and pChop [29–32]. Each of these ribozyme cassettes consists of two *cis*-acting ribozymes, designed to autocatalytically liberate the *HnudC*-targeted internal ribozyme. Both pClip and pChop allow the insertion of two contiguous transacting internal hammerhead ribozymes, whose activities do not adversely affect each other [32]. Thus,

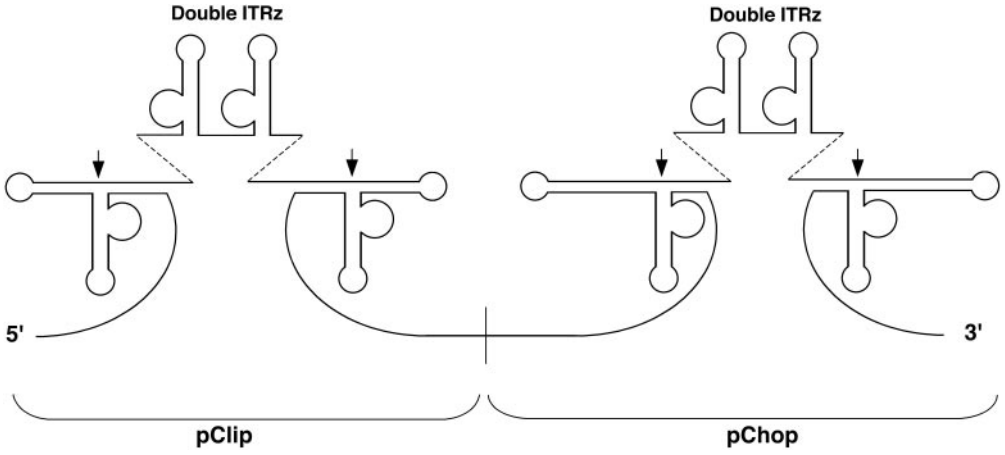

FIG. 1. Diagrammatic representation of pSNIP. Parent double ribozyme cassette (pClip and pChop), consisting of 5′ and 3′ *cis*-acting ribozymes flanking internal cloning sites, were ligated. The *HnudC*-targeted internal ribozymes were synthesized and ligated into pClip at *Bgl*II and *Mfe*I sites and into pChop at *Bam*HI and *Eco*RI sites, and the orientation was verified by DNA sequencing.

four internal ribozymes, which target *HnudC* mRNA, can be encoded in pSNIP (a schematic representation of pSNIP is shown in Fig. 1).

A library selection technique [33], modified from that described by Leiber and Strauss [34], was used to select optimal target sites on *HnudC* mRNA for the *HnudC* ribozyme. After six rounds of selection (described under Materials and Methods), six consensus high affinity-binding sites for the *HnudC*-targeted ribozymes were identified which contained internal -TC- sites (Table 1). Oligonucleotides containing a 5′ region of 16 fixed nucleotides (including the T7 promoter), a region of 6 *HnudC* sequence-specific nucleotides, a -GA-, another region of 9 specific nucleotides, and then another 3′ region of 15 fixed nucleotides (16-N_6-GA-N_9-15) were synthesized for each of the six internal ribozyme sequences.

We tested the ability of the *HnudC*-targeted ribozymes identified by library selection to cleave target *HnudC* RNA *in vitro*. ^{32}P-labeled *HnudC* RNA was prepared by *in vitro* transcription. Unlabeled *HnudC* internal ribozymes were synthesized *in vitro* using the T7 promoter. The ^{32}P-labeled *HnudC* RNA was incubated in the presence or the absence of internal ribozymes for 80 min and the products were then examined by SDS–PAGE followed by autoradiography. The best target cleavage was obtained with ribozymes targeted to the sites designated 2, 3, 4, and 6 (Fig. 2). No cleavage was observed when target RNA was incubated without internal ribozyme (control). Cleavage of the 1.29-kb target *HnudC* RNA produced the expected fragments of 133 and 1157 bases (ribozyme cleavage site 2), 159 and 1131 bases (site 3), 658 and 632 bases (site 4), and 724 and 566 bases (site 6). In these exper-

TABLE 1

Localization of Ribozyme High-Affinity Binding Sites within *HnudC* mRNA

Ribozyme		Sequence						Location on *HnudC* mRNA
1	T	5′ GGA	CGT	GGA	TC	GGA	GCC 3′	−23 to −7
	R	3′ CCT	GCA	CCT	AG	CCT	CGG 5′	
2	T	5′ AGG	AGC	GGT	TC	GAC	GGC 3′	20 to 36
	R	3′ TCC	TCG	CCA	AG	CTG	CCG 5′	
3	T	5′ GGC	CAT	GGC	TC	AGC	AGC 3′	46 to 61
	R	3′ CCG	GTA	CCG	AG	TCG	TCG 5′	
4	T	5′ ACC	TGG	CGG	TC	CCT	TTC 3′	545 to 561
	R	3′ TGG	ACC	GCC	AG	GGA	AAG 5′	
5	T	5′ TGG	TGG	ACA	TC	CAG	CGG 3′	596 to 612
	R	3′ ACC	ACC	TGT	AG	GTC	GCC 5′	
6	T	5′ GGC	GGC	ACC	TC	CGG	GTG 3′	611 to 627
	R	3′ CCG	CCG	TGG	AG	GCC	CAC 5′	

Note. T indicates a sequence on *HnudC* mRNA and R indicates a *HnudC*-targeted ribozyme sequence. High-affinity binding sites were identified by library selection and are numbered based on their relative distance from the translation initiation codon.

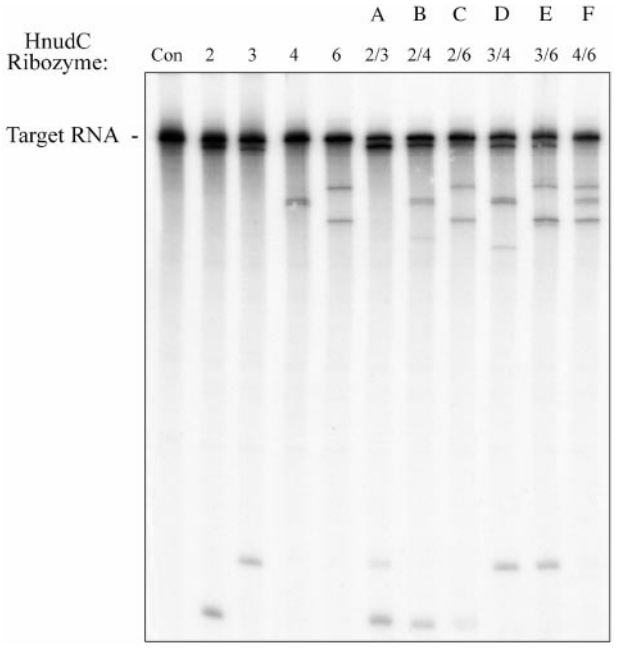

FIG. 2. *In vitro* target cleavage of *HnudC* RNA by internal ribozymes. Ribozymes are numbered by the *HnudC* sites they target and consist of one single (sites 2, 3, 4, and 6) or two (double constructs designated A to F) internal ribozymes. The control (con) was incubated without internal ribozyme.

iments, conditions for cleavage of target RNA including ribozyme to target ratio or time of incubation were not optimized to cleave all target since the objective of these *in vitro* experiments was to demonstrate correct cleavage with appropriately sized products.

The single internal *HnudC*-targeted ribozymes 2, 3, 4, and 6 were also produced as contiguous pairs, to create the double internal ribozymes 2/3, 2/4, 2/6, 3/4, 3/6, and 4/6. Results (Fig. 2) demonstrate efficient cleavage and absence of inhibition when two transacting internal ribozymes are contiguous. Target cleavage efficiency of these double internal ribozymes was at least two times higher than that with single ribozymes, measured by densitometric quantification of the residual labeled *HnudC* target mRNA following ribozyme incubation (not shown). The double internal ribozymes 2/3, 3/4, 3/6, and 4/6, which showed the greatest activity *in vitro,* were then subcloned into pSNIP at *Bam*HI/*Eco*RI (pChop) and *Bgl*II/*Mef*I (pClip) sites, respectively (see Fig. 1). These pSNIP constructs were designated A (contains two 2/3), D (contains two 3/4), E (contains two 3/6), and F (contains two 4/6).

To document self-liberation of the double internal ribozymes, all four *HnudC* double ribozyme oligonucleotides (A, D, E, and F in pSNIP) were cloned into the pCRII vector (Invitrogen) at *Hin*dIII/*Xba*I sites and then amplified using M13 primers by PCR. Sense transcripts were produced with the Sp6 polymerase and antisense transcripts with the T7 polymerase. After transcription and incubation for 5–50 min, RNA was analyzed by PAGE (Fig. 3). Time-dependent liberation of the internal ribozyme was demonstrated for the sense Sp6 transcript, whereas for the antisense transcript (T7), no cleavage was detected (Fig. 3A). Significant release of the internal ribozyme was observed even at 5 min. Similar results were observed with all four double *HnudC* internal ribozymes (Fig. 3B), documenting self-liberation of the internal ribozymes *in vitro* from the *HnudC*-targeted ribozyme cassette pSNIP.

Induction of HnudC-Targeted Ribozymes in Stably Transfected 293 Cells Inhibits Cell Proliferation

HnudC triple ribozymes A, D, and E in the pSNIP cassette were cloned into the multiple cloning site of pIND, the expression plasmid of the ecdysone system containing a modified ecdysone response element upstream of a minimal heat shock promoter. This was done using primers incorporating restriction sites compatible with the pIND vector's cloning sites and PCR to amplify the pSNIP triple ribozymes using high fidelity

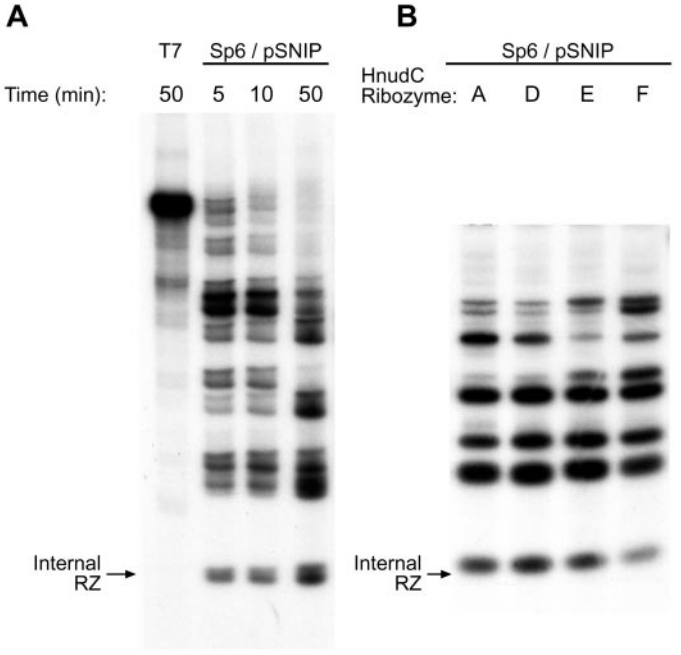

FIG. 3. *In vitro* self-liberation of the *HnudC*-targeted internal ribozymes. (A) Sense transcripts (Sp6 polymerase) and antisense transcripts (T7) were produced from M13 primer-amplified pCRII pSNIP *HnudC* double internal ribozyme A (cleavage sites 2 and 3). Transcripts were incubated for 5, 10, or 50 min prior to SDS–PAGE. Time-dependent liberation of the sense internal ribozyme is demonstrated and the internal ribozyme A (RZ) is indicated. No self-liberation was observed with antisense T7 transcript. (B) Self-liberation of the pSNIP *HnudC*-targeted internal ribozymes A, D, E, and F is shown after 50 min of incubation.

Vent polymerase. All constructs were sequenced to confirm their identity. In the pIND system, the ecdysone receptor (VgEcR) and the retinoid X receptor (RXR) are expressed from pVgRXR. Addition of muristerone A induces heterodimer formation of RXR and VgEcR, which then binds the hybrid ecdysone response element on pIND. Transcription of the gene of interest, in this case the pSNIP ribozyme cassette, is thus activated. Kidney 293 cells stably expressing pVgRXR were transfected with pIND-SNIP constructs containing the double internal ribozymes A, D, or E. Double internal ribozyme F was not pursued since liberation of the internal ribozyme was not as efficient as that for constructs A, D, and E (see Fig. 3B). However, pilot studies were performed on 293 cells stably expressing pIND-SNIP constructs containing double internal ribozyme F, targeted to cleavage sites 4 and 6. The effect on cell proliferation was similar to that observed with ribozymes A, D, and E. As a control for nonspecific effects, cells were also transfected with pIND-SNIP without internal ribozyme, designated construct S. Stably transfected clones for each of the constructs were isolated by antibiotic selection. We initially screened transfectants for 11 different S clones, 5 A clones, 13 D clones, 15 E clones, and 16 F clones. Since it was not feasible to study this number of clones, six representative transfectants were selected for detailed analysis.

To examine the influence of *HnudC*-targeted triple ribozyme induction on cell proliferation, stably transfected 293 cells were plated at a density of 500 cells/well in 0.5 ml of Dulbecco's media and 2 μM muristerone A (or the same volume of vehicle) was added on days 2–11. For these experiments, clones were transfected with pIND-SNIP alone (clones S7, S10) or pIND-SNIP containing *HnudC*-targeted internal ribozyme constructs A (clones A7, A18), D (clone D6), or E (clone E6). Wells were trypsinized and cells were counted in duplicate or triplicate from days 5 to 11. Results (Fig. 4) demonstrate significant and specific inhibition of cell proliferation following induction of *HnudC*-targeted ribozyme expressing clones, but not in uninduced cells or cells transfected with the pIND-SNIP alone. These growth experiments were repeated five times with similar results and are representative of all clones studied with each construct. When clones S7 or S10 (pIND-SNIP alone) were cultured with or without muristerone A to induce ribozyme expression, no inhibition of cell proliferation was observed. Differences observed in ribozyme induced cells were more significant at later days of culture. This may occur because cells with downregulated *HnudC* mRNA stop proliferating, while control cells continue to divide or because HNUDC has a long half life and is reduced by cell division rather than by rapid turnover, leading to a delay until effects can be observed. In Fig. 5, photographs of representative sections of uninduced and induced cultures at day 10 are shown. For clone S7, the appearance of cultures at days 10–11 was similar to that for S10 and for A7 and A18 was similar to that for D6 and E6.

To examine the mechanism of decreased proliferation in ribozyme-induced cells, cells were counted with trypan blue. No increase in dead cells, which failed to exclude trypan blue, was observed in ribozyme-induced cells compared to control cells examined at days 5–11. No difference in the number of nonadherent cells in the supernatant was observed between ribozyme-induced and uninduced cells. These data suggest that the decrease in cell number was not due to decreased cell viability or a change in the adherence characteristics of the cells. Western blotting was also performed on cells removed from culture on day 5 or 8 after exposure to muristerone A. Blots were probed with antibodies to PARP, caspase 8, and caspase 3. No differences in the quantities of these proteins or their cleavage products were observed between ribozyme-induced and uninduced cells. We also performed cell cycle analysis on uninduced or induced cells at day 5 or 11, stained with propidium iodide. No differences in the cell cycle profiles were observed between induced and uninduced cells. In summary, no decrease in cell viability, increase in apoptosis, or cell cycle arrest was observed in cells in which the *HnudC* ribozyme was induced. Although a mechanism for decreased cell proliferation was not identified, prolongation of the cell cycle without arrest is a postulated explanation of these observations.

HnudC-Targeted Triple Ribozyme Induction Results in Reduced HnudC mRNA Expression

To examine muristerone-A-induced ribozyme expression and target RNA inhibition, RNA was isolated from transfected cell lines induced by muristerone A and analyzed with dot blots. Blots were first probed with labeled inserts from *HnudC* ribozyme constructs A, D, and E to detect ribozyme induction, followed by stripping and reprobing with a labeled *HnudC* probe and GAPDH as a control for loading. Results (Fig. 6) demonstrate time-dependent induction of the *HnudC* ribozyme for clones A18, D6, and E6. Little induction was demonstrated with the pIND-SNIP control without internal ribozyme (S7); this may be due to reduced stability of the pSNIP ribozyme cassette without internal ribozyme. *HnudC* mRNA levels measured following induction by densitometric quantification of dot blots demonstrated decreases in HnudC mRNA levels to 70% compared with levels observed prior to induction of the *HnudC*-targeted ribozyme for clones A18, D6, and E6 (Fig. 6). Induction of the S7 clone was without significant effects on *HnudC* mRNA levels. These data demonstrate the efficacy of the *HnudC*-

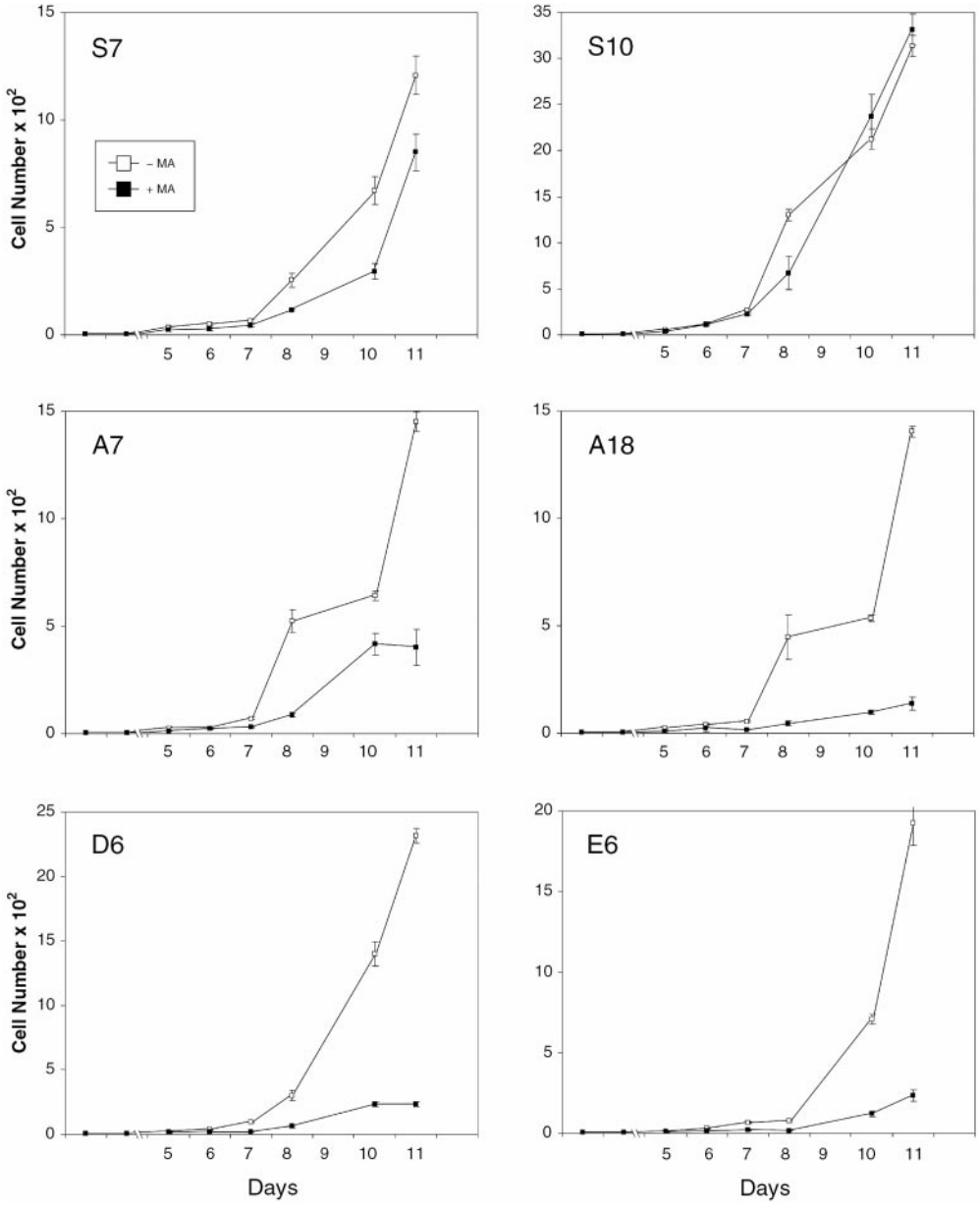

FIG. 4. *HnudC* ribozyme induction inhibits proliferation of 293 cells; 293 cells stably transfected with pIND-SNIP containing *HnudC*-targeted ribozymes (constructs A, D, and E) or pIND-SNIP alone (S) were induced (+) or uninduced (−) with muristerone A (2 μM) on days 2–11 and cells counted on days 5–11. Prior to day 5, the cell number was too low to reproducibly assess. Mean ± SEM cell number from triplicate plates is shown for one experiment. Clones studied were A7, A18, D6, and E6, in which pIND-SNIP contained *HnudC*-targeted internal ribozymes, or the S7 and S10 control clones transfected with pIND-SNIP alone. Results are representative of five experiments.

targeted ribozyme in cell culture. They also show that significant reduction in *HnudC* mRNA is associated with dramatic loss of proliferative capacity, even if residual *HnudC* mRNA remains.

Induction of the HnudC-Targeted Ribozyme Results in Multipolar Spindles in Mitotic Cells

Because ribozyme-mediated inhibition of *HnudC* function caused marked effects on cell proliferation, and this protein may influence cytoplasmic dynein, we investigated the effects of lack of *HnudC* function on mitotic spindle formation. Clones A18, D6, and E6, along with control clone S7, were cultured for a period of 7 days with and without addition of muristerone A as described above. Cells were subsequently fixed and stained to reveal microtubule architecture using an antibody directed against α-tubulin and DAPI staining to visualize DNA.

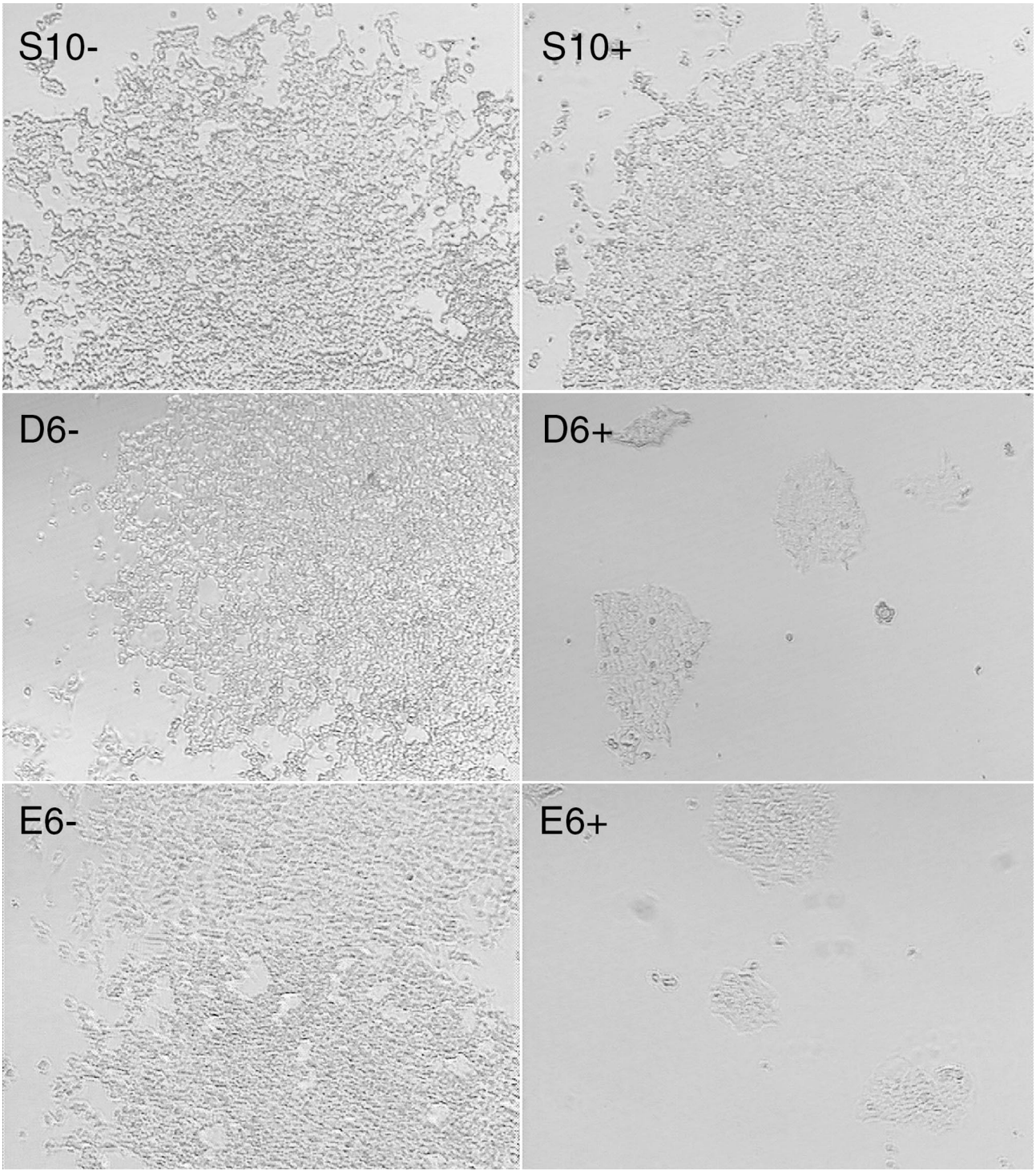

FIG. 5. Kidney embryonic 293 cells transfected with pIND-SNIP alone (clone S10) or pIND-SNIP *HnudC*-targeted internal ribozyme constructs (clones D6 and E6) were cultured with (+) or without (−) the inducer muristerone A for 10 days and then photographed.

Normal bipolar spindles were observed during mitosis in the majority of mitotic cells during growth of clones A18, D6, and E6 in the absence of muristerone addition. A similar situation was also seen in the S7 control cells, whether grown with or without the addition of muristerone A (data not shown). However, for the clones expressing the anti-*HnudC* ribozymes, many mitotic cells displayed defects in spindle archi-

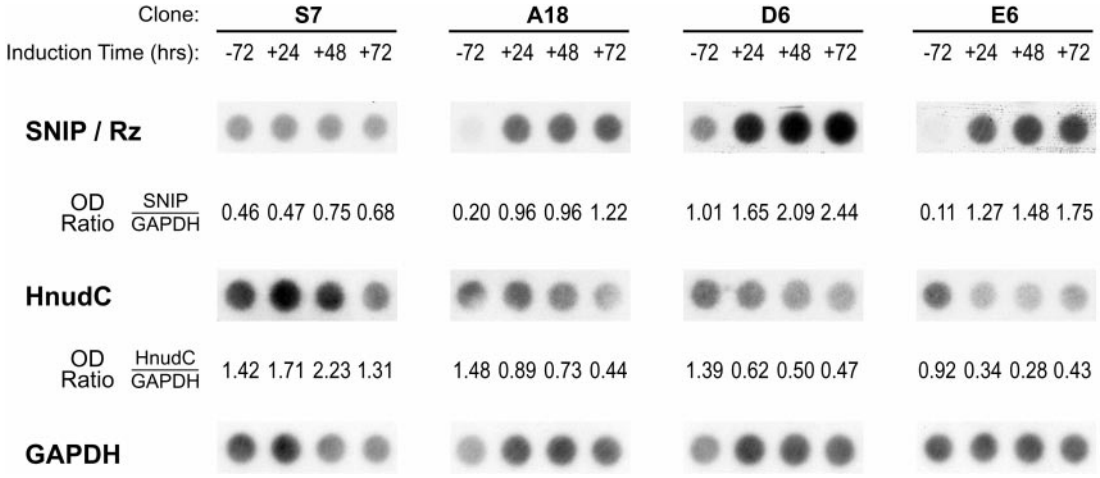

FIG. 6. Induction of *HnudC*-targeted ribozyme expression and influence on *HnudC* mRNA in transfected 293 cells. RNA was prepared from cells transfected with pIND-SNIP containing *HnudC*-targeted internal ribozymes (clones A18, D6, and E6) 72 h prior to and following induction with muristerone A for 24, 48, or 72 h. RNA was also prepared from the S7 control clone transfected with pIND-SNIP alone. Dot blots were prepared by exposure to labeled probes for SNIP (S7) or SNIP with internal ribozyme (A, D, and E). Blots were then stripped and reprobed for detection of *HnudC* mRNA, followed by reprobing for GAPDH. Densitometry measurements are shown as the ratio of the OD measured for pSNIP or *HnudC* mRNA divided by the GAPDH measurement to compensate for loading differences. Experiments were repeated twice with similar results. The observed decreases in *HnudC* mRNA levels were 54–70% normalized to GAPDH levels.

tecture during mitosis (Table 2). By far the most common defect observed was tripolar or tetrapolar mitotic spindles containing more than two spindle organizing centers (Fig. 7). Consistent with this observation, a fourfold increase in multinuclearity was also observed at day 7 in induced compared to uninduced cells in three independent experiments. Since specific induction of ribozymes to *HnudC* mRNA caused marked mitotic defects, these data indicate that inhibition of *HnudC* function affects normal spindle formation.

DISCUSSION

These experiments demonstrate that downregulation of *HnudC* mRNA by an inducible *HnudC*-targeted triple ribozyme *in vivo* results in dramatic inhibition of cellular proliferation. Analysis of three different *HnudC*-targeted internal ribozyme constructs confirmed these results. Clones transfected with double ribozyme cassettes (pSNIP) without the *HnudC*-targeted internal ribozyme showed a normal growth rate,

TABLE 2

Abnormal Mitotic Spindle Formation Following *HnudC*-Targeted Ribozyme Induction

	Percentage of abnormal spindles	
Clone	Control	Induction
S7	2.0 ± 0.3	1.3 ± 0.6
A18	2.6 ± 0.4	17.9 ± 1.1*
D6	1.3 ± 0.6	19.8 ± 0.6*
E6	1.0 ± 0.7	16.5 ± 1.8*

Note. The percentage of abnormal mitotic spindles is shown for clones S7, A18, D6, and E6 in cultures uninduced (control) or induced with muristerone A to express ribozymes to *HnudC* mRNA for 7 days. A minimum of 250 mitotic cells were examined for each uninduced and induced clone.

* Indicates a significant difference between uninduced and induced cells ($P < 0.01$).

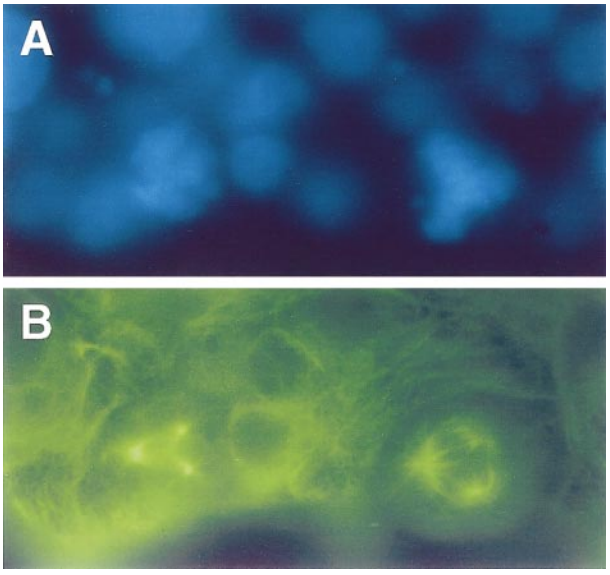

FIG. 7. Multipolar spindles form in mitotic cells following *HnudC* ribozyme induction. Clone E6 cells were grown for 7 days with muristerone A to induce expression of *HnudC* triple ribozymes. Cells were fixed and processed for DAPI staining (A) to reveal DNA and with α-tubulin antibodies (B) to show microtubules. Here, representative defects are shown in two cells in mitosis with tripolar spindles, with the mitotic cell at right clearly trying to segregate DNA in three directions at metaphase.

even in the presence of inducer, demonstrating absence of nonspecific toxicity of muristerone A and/or the ribozyme cassette. These data in human cells are consistent with those previously observed in *A. nidulans*, where deletion of *nudC* profoundly affected nuclear migration, colony growth, and cell wall composition [18].

These functional studies demonstrate a critical role for *HnudC* in eukaryotic cell proliferation and confirm our previous work with phosphorothioate antisense oligonucleotides targeted to *HnudC* mRNA [26]. This is consistent with previous studies with human [25] and murine [38] tissue demonstrating high expression in more rapidly proliferating normal tissues and a correlation in murine prostate tumors [38] and human leukemia samples [26] between NUDC expression and tumor aggressiveness. In *A. nidulans*, many of the currently identified *nud* loci encode either dynein or a protein which interacts with it [3, 8–16, 21]. Cytoplasmic dynein is a complex, minus end-directed microtubule motor which functions in vesicle transport and in mitosis to regulate spindle assembly, spindle orientation, centrosome separation as well as nuclear migration [4, 5, 8, 10, 11, 15, 16, 35–37]. Dynactin is required for most or all dynein-mediated activities [15, 16]. Microinjection of antidynein antibodies caused disruption of mitotic spindle formation in mammalian cells [36], as did overexpression of the dynamitin subunit of dynactin [37]. Current data suggest that microtubule tethering to spindle poles is mediated by a large complex containing dynein, dynactin, and NuMA, in which dynein motor activity powers the complex toward microtubule minus ends and dynactin and NuMA provide crosslinking [15]. In spindle assembly, both dynein and dynactin also interact at the kinetochore [16]. Overexpression of LIS-1 (*nudF*) resulted in multipolar mitotic spindles, unaligned chromosomes, and micronuclei/multiple nuclei and injection of antibody to deplete LIS-1 also interfered with spindle formation and lead to chromosome loss, demonstrating that expression of LIS-1 in a narrow range is critical for normal mitosis [8]. Both dynein and dynactin co-immunoprecipitate with LIS-1 and overexpression of LIS-1 alters the distribution of cytoplasmic dynein and dynactin [8]. These data, and those from others [11, 13], strongly suggest that LIS-1 and the newly identified human homolog of *nudE* are important in the localization of cytoplasmic dynein heavy chain and in the regulation of dynein motor function.

Our antitubulin immunofluorescence studies in cells with reduced *HnudC* expression show that *HnudC* is also required in spindle assembly. These data, establishing an essential role for HNUDC in mitotic spindle formation, lead us to speculate that, like homologs of other fungal nuclear migration genes, *HnudC* is involved in the interaction between centrosomes and microtubules and that it may affect dynein function during mitosis. Although our data demonstrate a role of *HnudC* in mitotic spindle formation and cell division, whether HNUDC directly interacts with dynein, dynactin, or LIS-1/nudE or through control of LIS-1 expression [6] requires further investigation. Since we have previously shown high levels of HNUDC expression in secretory and ciliated cells, HNUDC may have other roles, in addition to involvement in mitotic spindle formation, where its function may also involve an interaction with dynein, microtubules, or microtubule-organizing centers.

Our results here document triple ribozyme efficacy in an inducible system *in vivo*, which produces a decline in target mRNA (*HnudC*). The dramatic inhibition of growth produced by the *HnudC*-targeted triple ribozymes was not associated with complete loss of *HnudC* mRNA. However, given the dramatic effects on mitotic spindle formation, we hypothesize that the culture selects for cell populations expressing relatively low levels of the triple ribozyme (that is, higher expression levels produce abnormal mitoses and decreased proliferation). In fact, our data strongly suggest that *HnudC* is essential and that cells expressing limiting amounts of *HnudC* are unable to proliferate. Therefore, we hypothesize that it will be impossible to obtain a culture of cells in which expression of *HnudC* is reduced below a certain threshold level required for continued growth.

This study demonstrates the utility of the triple ribozyme approach to specifically modulating the function of essential genes. In the triple ribozyme approach, two *cis*-acting ribozymes efficiently release the targeted internal ribozyme with minimal nonspecific flanking sequences. The liberated internal targeted ribozyme shows substantially greater catalytic activity than single ribozymes with bilateral flanking vector sequences or than constructs that cannot undergo self-liberation [29]. This enables release of the targeted ribozyme within the nucleus so that the targeted mRNA can be inactivated before it can be translated [30, 31]. Triple ribozyme constructs driven by tissue-specific promoters have resulted in selective gene knockout. For example, a triple ribozyme targeted to an RNA polymerase I subunit, whose expression was driven by the prostate-specific probasin promoter, selectively ablated prostate epithelium [39]. Targeted downregulation of *HnudC* using triple ribozyme constructs driven by tissue-specific promoters may be useful in the future as an approach to therapy of malignancies, including leukemia, because the level of HNUDC was greatly increased in marrow aspirates from patients with acute lymphoblastic leukemia and acute myelogenous leukemia [26]. Importantly, our studies suggest that complete elimination of *HnudC*

mRNA is not required to significantly impact proliferation.

Genetic instability is a common feature of malignant tumors, characterized by an abnormal number of chromosomes (aneuploidy). Defects in chromosome number are thought to occur through missegregation of chromosomes, which may result from defects in mitotic organization [40–42]. Manipulation of levels of several proteins/complexes involved in spindle pole formation (dynein, dynactin, NuMA, and LIS-1), through depletion by microinjection of antibodies or overexpression, has been shown to result in multipolar spindles and/or unaligned chromosomes [8, 13–16, 36, 37]. Hence, expression of these components in a critical range is required for normal spindle formation and chromosomes segregation. Here, we report that the level of the human homolog of *nudC* is also critical in spindle pole formation and that depletion of *HnudC* disrupts normal spindle assembly.

The authors thank Tina Eberly and Julie A. Brosius for careful preparation of the manuscript and Carol Stine for technical assistance. This work was supported by National Institutes of Health Grants DK 46778 (B.A.M.), M01 RR10732 (GCRC Grant), F32 DK09790-03 (M.-Y.Z.), and GM 42564 (S.A.O.) and by the Four Diamonds Fund.

REFERENCES

1. Xiang, X., Osmani, A. H., Osmani, S. A., Roghi, C. H., Willins, D. R., Beckwith, S., Goldman, G., Chiu, Y., Xin, M., Liu, B., and Morris, N. R. (1995). Analysis of nuclear migration in *Aspergillus nidulans*. *Cold Spring Harbor Symp. Quant. Biol.* **LX,** 813–819.
2. Morris, N. R. (2000). Nuclear migration. From fungi to the mammalian brain. *J. Cell Biol.* **148,** 1097–1101.
3. Xiang, X., Zuo, W., Efimov, V. P., and Morris, N. R. (1999). Isolation of a new set of Aspergillus nidulans mutants defective in nuclear migration. *Curr. Genet.* **35,** 626–630.
4. Xiang, X., Beckwith, S. M., and Morris, N. R. (1994). Cytoplasmic dynein is involved in nuclear migration in *Aspergillus nidulans*. *Proc. Natl. Acad. Sci. USA* **91,** 2100–2104.
5. Beckwith, S. M., Roghi, C. H., Liu, B., and Morris, N. R. (1998). The "8-kD" cytoplasmic dynein light chain is required for nuclear migration and for dynein heavy chain localization in *Aspergillus nidulans*. *J. Cell Biol.* **143,** 1239–1247.
6. Xiang, X., Osmani, A. H., Osmani, S. A., Xin, M., and Morris, N. R. (1995). *NudF*, a nuclear migration gene in *Aspergillus nidulans*, is similar to the human LIS-1 gene required for neuronal migration. *Mol. Biol. Cell* **6,** 297–310.
7. Reiner, O., Carrozzo, R., Shen, Y., Wehnert, M., Faustinella, F., Dobyns, W. B., Caskey, C. T., and Ledbetter, D. H. (1993). Isolation of a Miller-Dieker lissencephaly gene containing G protein β-subunit-like repeats. *Nature* **364,** 717–721.
8. Faulkner, N. E., Dujardin, D. L., Tai, C.-Y., Vaughan, K. T., O'Connell, C. B., Wang, Y.-L., and Vallee, R. B. (2000). A role for the lissencephaly gene *LIS1* in mitosis and cytoplasmic dynein function. *Nature Cell Biol.* **2,** 784–791.
9. Liu, Z., Steward, R., and Luo, L. (2000). Drosophila *Lis1* is required for neuroblast proliferation, dendritic elaboration and axonal transport. *Nature Cell Biol.* **2,** 776–783.
10. Smith, D. S., Niethammer, M., Ayala, R., Zhou, Y., Gambello, M. J., Wynshaw-Boris, A., and Tsai, L.-H. (2001). Regulation of cytoplasmic dynein behaviour and microtubule organization by mammalian Lis1. *Nature Cell Biol.* **2,** 765–767.
11. Wynshaw-Boris, A., and Gambello, M. J. (2001). LIS1 and dynein motor function in neuronal migration and development. *Genes Dev.* **15,** 639–651.
12. Efimov, V. P., and Morris, N. R. (2000). The LIS1-related NUDF protein of *Aspergillus nidulans* interacts with the coiled-coil domain of the NUDE/RO11 protein. *J. Cell Biol.* **150,** 681–688.
13. Sasaki, S., Shionoya, A., Ishida, M., Gambello, M., Yingling, J., Wynshaw-Boris, A., and Hirotsune, S. (2000). A LISI/NUDEL/cytoplasmic dynein heavy chain complex in the developing and adult central nervous system. *Neuron* **28,** 681–696.
14. Kitagawa, M., Umezu, M., Aoki, J., Koizumi, H., Arai, H., and Inoue, K. (2000). Direct association of LIS1, the lissencephaly gene product, with a mammalian homologue of a fungal nuclear distribution protein, rNUDE. *FEBS Lett.* **479,** 57–62.
15. Merdes, A., and Cleveland, D. W. (1997). Pathways of spindle pole formation: different mechanisms: Conserved components. *J. Cell Biol.* **138,** 953–956.
16. Karki, S., and Holzbaur, E. L. F. (1999). Cytoplasmic dynein and dynactin in cell division and intracellular transport. *Curr. Opin. Cell Biol.* **11,** 45–53.
17. Osmani, A. H., Osmani, S. A., and Morris, N. R. (1990). The molecular cloning and identification of a gene product specifically required for nuclear movement in *Aspergillus nidulans*. *J. Cell. Biol.* **111,** 543–551.
18. Chiu, Y., Xiang, X., Dawe, A. L., and Morris, N. R. (1997). Deletion of *nudC*, a nuclear migration gene of *Aspergillus nidulans*, causes morphological and cell wall abnormalities and is lethal. *Mol. Biol. Cell* **8,** 1735–1749.
19. Miller, B. A., Zhang, M.-Y., Gocke, C. D., DeSouza, C., Osmani, A. H., Lynch, C., Davies, J., Bell, L., and Osmani, S. A. (1998). A homolog of the fungal nuclear migration gene *NudC* is involved in normal and malignant human hematopoiesis. *Exp. Hematol.* **27,** 742–750.
20. Matsumoto, N., and Ledbetter, D. H. (1999). Molecular cloning and characterization of the human NUDC gene. *Hum. Genet.* **104,** 498–504.
21. Morris, S. M., Albrecht, U., Reiner, O., Eichele, G., and Yu-Lee, L. Y. (1998). The lissencephaly gene product Lis1, a protein involved in neuronal migration, interacts with a nuclear movement protein, NudC. *Curr. Biol.* **7,** 603–606.
22. Morris, S. M., Anaya, P., Xiang, X., Morris, N. R., May, G. S., and Yu-Lee, L.-Y. (1997). Prolactin-inducible T cell gene product is structurally similar to the *Aspergillus nidulans* nuclear movement protein NUDC. *Mol. Endocrinol.* **11,** 229–236.
23. Axtell, S. M., Truong, T. M., O'Neal, K. D., and Yu-Lee, L.-Y. (1995). Characterization of a prolactin-inducible gene, clone 15, in T cells. *Mol. Endocr.* **9,** 312–318.
24. Cunniff, J., Chiu, Y.-H., Morris, N. R., and Warrior, R. (1997). Characterization of *DnudC*, the *Drosophila* homolog of an *Aspergillus* gene that functions in nuclear motility. *Mech. Dev.* **66,** 55–68.
25. Gocke, C. D., Osmani, S. A., and Miller, B. A. (2000). The human homologue of the *Aspergillus* nuclear migration gene *nudC* is preferentially expressed in dividing cells and ciliated epithelia. *Histochem. Cell Biol.* **114,** 293–301.
26. Gocke, C. D., Reaman, G. H., Stine, C., Zhang, M.-Y., Osmani, S. A., and Miller, B. A. (2000). The fungal migration gene NUDC and human hematopoiesis. *Leukemia Lymphoma* **39,** 447–454.

27. James, H. A., and Gibson, I. (1998). The therapeutic potential of ribozymes. *Blood* **91,** 371–382.

28. Taira, K., Nakagawa, K., Nishikawa, S., and Furukawa, K. (1991). Construction of a novel RNA-transcript-trimming plasmid which can be used both *in vitro* in place of run-off and (G)-free transcriptions and *in vivo* as multi-sequences transcription vectors. *Nucleic Acids Res.* **19,** 5125–5130.

29. Benedict, C. M., Pan, W., Loy, S. E., and Clawson, G. A. (1998). Triple ribozyme-mediated down-regulation of the retinoblastoma gene. *Carcinogenesis* **19,** 1223–1230.

30. Ren, L., Schalles, S. L., Pan, W., Isom, C. E., Loy, S. E., Lee, J.-H., Benedict, C. M., Pickering, M. T., Norris, J. S., and Clawson, G. A. (1998). Construction and deployment of triple ribozymes targeted to multicatalytic proteinase subunits C3 and C9. *Gene Ther. Mol. Biol.* **3,** 1–13.

31. Crone, T., Schalles, S., Benedict, C., Pan, W., Ren, L., Loy, S., Isom, H., and Clawson, G. (1999). Growth inhibition by a triple ribozyme targeted to repetitive B2 transcripts. *Hepatology* **29,** 1114–1123.

32. Clawson, G. A., Pan, W., Isom, H., Christensen, N., and Norris, J. S. (1999). Development of therapeutic ribozyme reagents directed against hepatitis B virus and human papillomavirus. *Int. J. Mol. Med.* **4**(Suppl.), S42.

33. Pan, W.-H., Devlin, H., Kelley, C., Isom, H., and Clawson, G. A. (2001). A selection system for identifying ribozyme target cleavage site accessibility. *RNA* **7,** 610–621.

34. Lieber, A., and Strauss, M. (1995). Selection of efficient cleavage sites in target RNAs by using a ribozyme expression library. *Mol. Cell. Biol.* **15,** 540–551.

35. Gönczy, P., Pichler, S., Kirkham, M., and Hyman, A. A. (1999). Cytoplasmic dynein is required for distinct aspects of MTOC positioning, including centrosome separation, in the one cell stage *Caenorhabditis elegans* embryo. *J. Cell Biol.* **147,** 135–150.

36. Vaisberg, E. A., Koonce, M. P., and McIntosh, J. R. (1993). Cytoplasmic dynein plays a role in mammalian mitotic spindle formation. *J. Cell Biol.* **123,** 849–858.

37. Echeverri, C. J., Paschal, B. M., Vaughan, K. T., and Vallee, R. B. (1996). Molecular characterization of 50 kD subunit of dynactin reveals function for the complex in chromosome alignment and spindle organization during mitosis. *J. Cell Biol.* **132,** 617–633.

38. Aumais, J. P., Tunstead, J. R., Morris, S. M., Yu-Lee, L.-Y. (2000). Upregulation of Nudc, but not Lis-1, expression correlates to the proliferative status of cells and tumors and may be involved in polarized cell function. *Mol. Biol. Cell (Suppl.)* **11,** 353a.

39. Voeks, D., Clawson, G., and Norris, J. (1998). Tissue-specific triple ribozyme vectors for prostate cancer gene therapy. *Gene Ther. Mol. Biol.* **1,** 407–418.

40. Pihan, G. A., and Doxsey, S. J. (1999). The mitotic machinery as a source of genetic instability in cancer. *Cancer Biol.* **9,** 289–302.

41. Pihan, G. A., Purohit, A., Wallace, J., Knecht, H., Woda, B., Quesenberry, P., and Doxsey, S. J. (1998). Centrosome defects and genetic instability in malignant tumors. *Cancer Res.* **58,** 3974–3985.

42. Doxsey, S. (1998). The centrosome—A tiny organelle with big potential. *Nature Genet.* **20,** 104–106.

Received May 31, 2001
Revised version reviewed October 12, 2001
Published online December 20, 2001